THE BRIKEN PROJECT: EXTENSIVE MEASUREMENTS OF β-DELAYED NEUTRON EMITTERS FOR THE ASTROPHYSICAL r PROCESS*

J.L. Tain[a], J. Agramunt[a], D.S. Ahn[b], A. Algora[a,c], J.M. Allmond[d]
H. Baba[b], S. Bae[e], N.T. Brewer[c], R. Caballero Folch[f], F. Calvino[g]
P.J. Coleman-Smith[h], G. Cortes[g], T. Davinson[i], I. Dillmann[f]
C. Domingo-Pardo[a], A. Estrade[j], N. Fukuda[b], S. Go[k,b], C. Griffin[i]
R. Grzywacz[k], J. Ha[e], O. Hall[i], L. Harkness-Brennan[l], T. Isobe[b], D. Kahl[i]
M. Karny[m], G.G. Kiss[c,b], M. Kogimtzis[h], A. Korgul[m], S. Kubono[b]
M. Labiche[h], I. Lazarus[h], J. Lee[n], J. Liu[n], G. Lorusso[o,b], K. Matsui[b,p]
K. Miernik[d,m], F. Montes[q], B. Moon[r], A.I. Morales[a], N. Nepal[j]
S. Nishimura[b], R.D. Page[l], Z. Podolyak[s], V.F.E. Pucknell[h], B.C. Rasco[d]
P.H. Regan[o,s], A. Riego[g], B. Rubio[a], K.P. Rykaczewski[d], Y. Saito[f]
H. Sakurai[b,p], Y. Shimizu[b], J. Simpson[h], P.A. Söderström[b], D.W. Stracener[d]
T. Sumikama[b], R. Surman[t], H. Suzuki[b], M. Takechi[u], H. Takeda[b]
A. Tarifeno-Saldivia[g], S.L. Thomas[v], A. Tolosa-Delgado[a]
V.H. Phong[z], P. Woods[i]

for the BRIKEN Collaboration

[a]Instituto de Fisica Corpuscular (CSIC–Universitat de Valencia), 46980 Paterna, Spain
[b]RIKEN Nishina Center, Wako, Saitama 351-0198, Japan
[c]Inst. of Nuclear Research, Hungarian Academy of Sciences, Debrecen Pf. 51, 4001, Hungary
[d]Physics Division, Oak Ridge National Laboratory, Oak Ridge, TN 37831, USA
[e]Dept. of Physics and Astronomy, Seoul National University, Seoul, 08826, Republic of Korea
[f]TRIUMF, 4004 Wesbrook Mall, Vancouver, British Columbia, V6T 2A3, Canada
[g]Universitat Politecnica de Catalunya (UPC), Barcelona, Spain
[h]STFC Daresbury Laboratory, Daresbury, Warrington WA4 4AD, UK
[i]University of Edinburgh, Edinburgh, EH9 3FD, UK
[j]Central Michigan University, Mount Pleasant, MI 48859, USA
[k]Dept. of Physics and Astronomy, Univ. of Tennessee, Knoxville, TN 37996-1200, USA
[l]University of Liverpool, Liverpool, L69 7ZE, UK
[m]Faculty of Physics, University of Warsaw, Pasteura 5, 02-093 Warszawa, Poland
[n]Department of Physics, The University of Hong Kong, Pokfulam Road, Hong Kong, China
[o]National Physical Laboratory, Teddington, UK TW11 0LW, UK
[p]Department of Physics, University of Tokyo, Hongo, Bunkyo-ku, Tokyo 113-0033, Japan
[q]National Superconducting Cyclotron Lab., Michigan State Univ., East Lansing, MI 48824, USA
[r]Department of Physics, Korea University, Seoul 136-701, Republic of Korea
[s]Department of Physics, University of Surrey, Guildford GU2 7XH, UK
[t]Department of Physics, University of Notre Dame, Notre Dame, IN 46556, USA
[u]Department of Physics, Niigata University, Niigata 950-2102, Japan
[v]STFC Rutherford Appleton Laboratory, Harwell Campus, Didcot, Oxfordshire, OX11 0QX, UK
[z]Department of Nuclear Physics, Faculty of Physics, VNU University of Science, Hanoi, Vietnam

(Received January 3, 2018)

* Presented at the XXXV Mazurian Lakes Conference on Physics, Piaski, Poland, September 3–9, 2017.

An ambitious program to measure decay properties, primarily β-delayed neutron emission probabilities and half-lives, for a significant number of nuclei near or on the path of the rapid neutron capture process, has been launched at the RIKEN Nishina Center. We give here an overview of the status of the project.

DOI:10.5506/APhysPolB.49.417

1. Introduction

Most of the nuclei formed during the initial stages of the rapid (r) neutron capture process will decay by β-delayed neutron (βn) emission. For these nuclei, the separation energy of one or more neutrons in the daughter nucleus S_{xn} is lower than the energy available for the decay Q_β, making the process energetically possible. The half-life $T_{1/2}$ of the decay determines the initial abundances of the nuclei along the reaction path. The decay of these nuclei towards stability is altered by the neutron emission process, since each neutron emitted reduces the final mass number A by one unit. In addition, the injection of fresh neutrons to the system, at the moment that the neutron density is rapidly decreasing, can have a significant effect on the neutron capture rate, increasing A by one unit per (n,γ) reaction [1, 2]. Thus, the probability of x-neutron emission per decay P_{xn} shapes the final abundance distributions. All of this underlines the importance of accurate decay data for βn emitters in r process abundance calculations. However, obtaining such data in the past has been hampered by the difficulty of accessing the relevant isotopes, far from the valley of β stability. In fact, reaction network calculations of the r process rely heavily on theoretical estimates for $T_{1/2}$ and P_{xn} as well as for other relevant quantities such as the capture cross sections $\sigma_{n\gamma}$ and masses.

From the astrophysics point of view, in spite of the advances since the general idea of the r process was laid out [3], there are still considerable uncertainties. It is not clear what are the exact conditions of the astrophysical environment such as temperature, neutron density, entropy, rotation speed and magnetic fields, that lead to a successful r process. Where such events actually take place is also unknown. Two sites have been actively investigated: (1) core-collapse supernova events (CCSN) occurring at the ends of the lives of massive stars, and (2) the kilonova explosion ignited by the merging of two neutron stars or a black hole and a neutron star (NSM). The relative contributions of the two to the evolution of the Universe and the observed abundances of elements in stars is also unclear. The very recent results of combined observations of gravitational wave, γ ray, X ray, UV, optical, infrared and radio emission from a two-neutron star merger confirm in a spectacular way that NSM are a major source of r process elements [4]

and opens a new field for precision r process studies. In this situation, it is fair to claim that a reduction in the uncertainty of the nuclear physics input, in particular for values of P_{xn} and $T_{1/2}$, is a key to the progress of investigations in this area.

With that idea in mind the Beta-delayed neutrons at RIKEN (BRIKEN) Collaboration [5] was established with the aim of exploiting the currently unsurpassed radioactive beam intensities by in-fight production available at the Radioactive Isotope Beam Factory (RIBF) [6] and the powerful selection and identification capabilities of the in-flight separator BigRIPS, and ZeroDegree spectrometer [7], by supplementing them with state-of-the-art instrumentation that would allow us to study decay properties of very exotic βn emitters.

2. Experimental setup

To determine neutron emission probabilities, we use a combination of neutron counting and β counting, a widely used method. The BRIKEN neutron counter is of the neutron moderation type, which uses a hydrogenous material, in our case high density polyethylene (HDPE), to bring down the neutron energy from MeVs to meVs, and a detector that is very efficient for detecting thermal neutrons, in our case a ^{3}He filled proportional counter. The energy deposited by the exothermic reaction $^3\mathrm{He}(n,p)^3\mathrm{H}$ ($Q = 0.76$ MeV) induces a signal well-separated from the noise and with a relatively small background, providing a high degree of selectivity. With this detection scheme, one can also reach high detection efficiencies by assembling a large number of tubes, a key feature for the study of weakly produced isotopes. The fraction of initial neutrons effectively moderated and captured depends on their initial energy and the geometry of the detector, resulting in an energy dependence of the neutron detection efficiency ε_n. This is an undesirable effect since the energy distribution is *a priori* unknown for most of the nuclei of interest. Thus, the arrangement of tubes to achieve maximum detection efficiency and minimum energy dependence is a complex problem that is best tackled using Monte Carlo (MC) simulations.

The optimization of the BRIKEN neutron counter was carried out using a parametric approach [8] taking into account the tubes available to the collaboration, coming from ORNL, UPC-Barcelona, GSI-Darmstadt, JINR and RIKEN, with varying gas volumes and pressures. One of the designs investigated includes γ-ray detectors, more specifically two CLOVER-type HPGe detectors. This option reduces the maximum achievable efficiency and flatness of the efficiency curve, but was the one chosen because of the enhanced research prospects provided by the significant gain in peak-to-background ratio of β-neutron gated γ-ray spectroscopy [9]. The CLOVER detectors are inserted perpendicular to the beam from opposite sides of the

PE moderator and achieve a γ-ray detection efficiency of about 3.5% for 1 MeV γ rays. The configuration finally installed includes 140 ^{3}He tubes (see Fig. 1, left panel), becoming the largest detector of its kind ever built for βn measurements, with a rather constant efficiency of around 68% up to 1 MeV, dropping to 59% at 3 MeV (see Fig. 1, right panel), according to MC simulations. Given the large energy window for βn emission in exotic neutron-rich nuclei, this variation can represent a source of systematic uncertainty in P_{xn} values. However, we can use the number of neutrons detected as a function of distance to the source, which carries information on the neutron energy as shown in the right panel of Fig. 1, to deduce *de facto* the average detection efficiency for each decaying nucleus [10]. The simulated neutron detection efficiency was verified with a strong uncalibrated ^{252}Cf source using the neutron multiplicity counting method [11]. Due to the close packing of ^{3}He tubes, the mean time for moderation and capture in ^{3}He is rather short, $\tau \sim 30$ μs. Thus, setting a time window for neutron detection of $\Delta t_n = 200$ μs ensures close to 100% detection efficiency. The signal from each tube, each HPGe crystal and other ancillary detectors is digitized when it goes above a noise discrimination threshold (self-triggering), processed with trapezoidal filters and stored in list-mode files as time-amplitude pairs, using the Gasific digital data acquisition system [12]. The resulting acquisition dead time is typically very small (less than 1%).

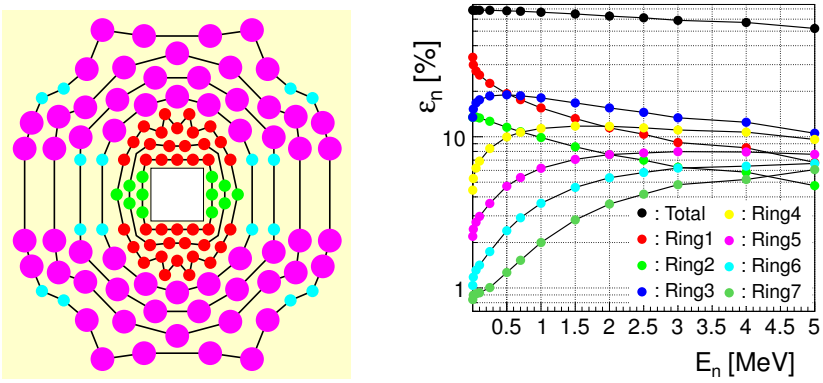

Fig. 1. (Color online) Left panel: Schematic lay-out of the ^{3}He tube distribution inside the HDPE moderator around the square shaped AIDA hole. The color indicates the tube type. Small medium-gray dots/green: $\oslash$ 1″ × 11.8″/5 atm — RIKEN; small dark-gray dots/red: $\oslash$ 1″ × 23.6″/8 atm — UPC; small light-gray dots/blue: $\oslash$ 1″ × 24″/10 atm — ORNL; big gray dots/pink: $\oslash$ 2″ × 24″/10 atm — ORNL. Tubes belonging to a single ring are connected with a line (Ring-1: innermost, Ring-7: outermost). Right panel: Neutron detection efficiency as a function of energy for each ring and the whole detector.

The β counter also acts as the ion implantation detector, namely the Advanced Implantation Detector Array (AIDA) [13]. A total of six Si DSSDs spaced by 10 mm were installed in the AIDA nose, which is inserted longitudinally in the PE moderator. The stack of DSSDs is centered with respect to the tubes and located between the two CLOVER detectors. Each DSSD has 1 mm thickness and a size of 72 mm $\times$ 72 mm with 128 horizontal and vertical strips on each side. Each strip is read out independently and processed with both high-gain and low-gain electronic branches. This allows one to measure precisely the low energy deposited by β signals shortly after an implantation event which deposits a very high energy. A threshold is applied to each electronic channel to discriminate against the noise and reduce data throughput. The threshold in the β branch ranges typically between 100 and 200 keV. The total data readout acquisition system stores the time and signal amplitude of all strips that fired.

The identification of each implanted ion is provided by the BigRIPS spectrometer. The ion velocity is measured by the time-of-flight between thin plastic scintillators located conveniently along the particle trajectory. The particle trajectory is reconstructed from the transverse position provided by two-dimensional parallel plate avalanche counters and combined with the magnetic field in the dipole magnets to obtain the particle's magnetic rigidity. Combining velocity and magnetic rigidity, one obtains the mass-over-charge ratio A/Q. The energy lost by the ion in dedicated ionization chambers provides its atomic charge Z. After identification of possible charge states (ions which are not fully stripped of electrons), the two quantities together provide a unique identification of the ion in an event-by-event basis.

The data from the three independent DACQ systems, BigRIPS, AIDA and BRIKEN, have to be merged for the data analysis. The merging is done on the basis of the respective time stamps which are synchronized thanks to the use of a common clock signal distributed to all three systems. The synchronization between them is constantly monitored during the measurement.

3. Experimental programme

Four measurement proposals have been approved until now. Altogether, they span a very wide range of very neutron-rich isotopes from Co to Eu (see Fig. 2). They cover the region of the 1$^{\text{st}}$ r process peak, Z = 27–35 and A = 75–95 [14], the region of neutron-rich deformed nuclei, Z = 35–48 and A = 95–130 [15], the region of the 2$^{\text{nd}}$ r process peak, Z = 45–55 and A = 120–150 [16], and the region of deformed nuclei leading to the rare-earth abundance peak (REP), Z = 55–63 and A = 150–167 [17]. The goal is to measure in total 135 new P_{1n} values, 85 new P_{2n} values and 40 new $T_{1/2}$ values for nuclei relevant to r process calculations.

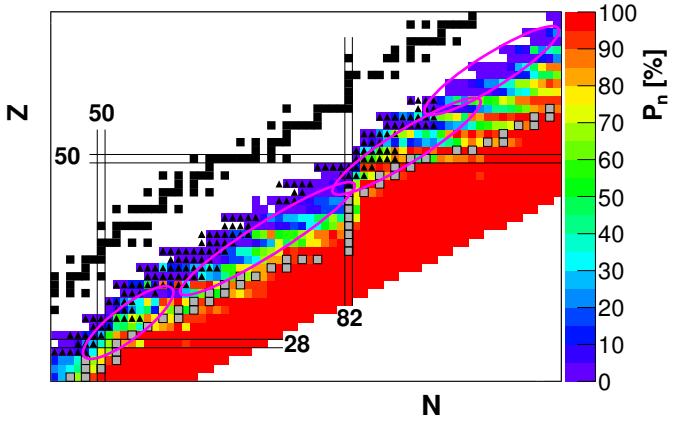

Fig. 2. (Color online) A plot of part of the nuclide chart showing calculated P_n values from Ref. [18] (color code on the right). Black triangles indicate isotopes where experimental information exists. Black squares indicate stable nuclei. Grey squares indicate waiting-point nuclei for a hot r process trajectory. The region of the chart covered by the four accepted BRIKEN proposals is roughly indicated by ellipses.

The physics reach of the expected results extends beyond the astrophysical interest. Half-lives and P_{xn} values give information on the β-strength distribution $S_\beta(E_x)$ which carries information on the nuclear structure. $T_{1/2}$ is mainly sensitive to the low excitation energy part of $S_\beta(E_x)$, while P_{xn} values measure the fraction of $S_\beta(E_x)$ above S_{xn}. The combined information provides constraints on the theoretical models calculating $S_\beta(E_x)$, thus improving their predictive power for nuclei as yet unmeasured. Alternatively, these two quantities together can provide information about the nuclear shell structure [19] or about the deformation of the nucleus [20, 21]. Additional nuclear structure information can come from the precise location of excited states and their βn feeding intensity obtained with the CLOVER γ-ray detectors. The background reduction provided by neutron gating [22, 23] will push the limit of such studies to more exotic nuclei.

The process of βn emission itself is not fully understood. For example, the competition between γ and neutron emission from neutron unbound states populated in β-decay has just started to be studied in a more systematic way [24–28]. The competition between β-delayed one-neutron and multiple-neutron emission channels has not been properly addressed [29], the main reason being the scarcity of known βxn emitters. Currently, only twenty three $\beta 2n$, four $\beta 3n$ and one $\beta 4n$ emitters have been measured. As mentioned above, we will substantially increase the database for $\beta 2n$ emitters providing the ground for an extensive systematic study. It is also un-

clear whether the multiple emission process occurs sequentially, or through the emission of a loosely bound neutron cluster, or as direct breakup into the continuum [30]. Some insight into this problem may be obtained by the measurement of angle-energy correlations between emitted neutrons, as has been done in the case of β-delayed proton emission [31]. Because of the neutron moderation process, the BRIKEN neutron counter can provide such information only with limitations. However, given its large neutron detection efficiency, it is worth to explore this possibility.

4. First measurements

The commissioning of the experimental setup took place in November 2016 parasitic to an experiment of M. Takechi and collaborators. The primary beam was ^{238}U at an energy of 345 MeV/u. The BigRIPS setting for the secondary radioactive beam was centered on ^{76}Ni. In about 10 hours of measurement, sufficient statistics were accumulated for 15 isotopes of Ni, Cu, Zn and Ga which are β-delayed one-neutron emitters. This includes 475 ^{78}Ni events, enough to determine its P_n value by direct neutron counting for the first time.

We observed a very large beam induced background in the neutron detector which reached a value of 250 cps (counts per second), to be compared with 0.4 cps from ambient background. This limits the sensitivity of our setup to β-delayed neutrons. A similar issue was found during the BELEN-30 experiment at the GSI Fragment Separator in 2011 [32]. There the problem was solved, for isotopes with low statistics and sufficient long half-life, using in the analysis only the decay data coming between beam spills. This is not possible at BigRIPS given the continuum time structure of the RIBF beams. However, we found that by vetoing neutrons coming within Δt_n (200 μs) of the passage of ions through the plastic scintillator at the end of the spectrometer, we effectively reduced the neutron detector background. Reduction factors of about 4 for the one-neutron background and about 15 for the two-neutron background were achieved. This procedure introduces a few percent beam-rate-dependent reduction on neutron statistics in the analysis.

In order to obtain the P_{1n} value we build for each identified implant the histogram of β-implant time differences, $t_\beta - t_{\text{implant}}$, both without any condition and with the condition that only one neutron comes within Δt_n after the β (see Fig. 3). These spectra are corrected for uncorrelated and correlated background and fitted with a function describing the evolution of the decay activity of parent and descendant nuclei for all decay chains. The fit function has the form of

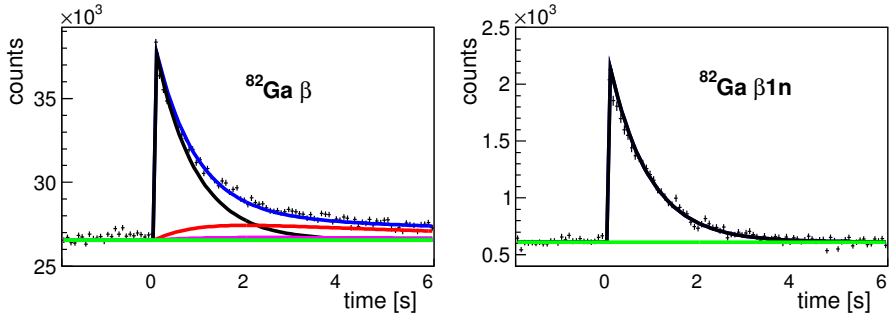

Fig. 3. (Color online) Time distribution of β signals with respect to implanted ^{82}Ga ions for the commissioning run. Left panel: without conditions. Right panel: neutron-gated. The uncorrelated background (in green) and the different decay components in the fit are shown (blue: sum of all contributions, black: ^{82}Ga, red: ^{82}Ge, pink: ^{81}Ge).

$$f(t) = \sum_i \bar{\varepsilon}_\beta^i \lambda_i N_i(t) + \sum_j \bar{\varepsilon}_\beta^j \bar{\varepsilon}_n^j P_{1n}^j \lambda_j N_j(t)\,, \tag{1}$$

where index i runs over all β decays, index j runs over all βn decays and $\lambda = \ln(2)/T_{1/2}$. The bar symbol above ε emphasizes that these efficiencies are average quantities, weighted with the corresponding β-intensity distribution. The number of decaying nuclei at each moment $N_k(t)$ is obtained from appropriate solutions of the Bateman equations [33] which take the form of

$$N_k(t) = N_1 \prod_{i=1}^{k-1} (b_{i,i+1}\lambda_i) \times \sum_{i=1}^{k} \frac{e^{-\lambda_i t}}{\prod_{j=1\neq i}^{k}(\lambda_j - \lambda_i)}\,, \tag{2}$$

where N_1 is the number of implanted parent ions and the branching ratio $b_{i,i+1}$ at the branching point i in the decay chain is either P_{1n}^i or $1 - P_{1n}^i$ depending on the branch. All half-lives and descendant P_{1n} values are kept fixed, thus a simultaneous fit of both histograms provides directly the neutron emission probability of the parent. The systematic uncertainty due to uncertainties on the $T_{1/2}$ and P_n values used is derived from the distribution of results obtained by repeated fitting after varying the parameters within uncertainties.

In the preliminary analysis, we assume that the neutron efficiency $\bar{\varepsilon}_n$ is isotope-independent. The common assumption that the efficiency $\bar{\varepsilon}_\beta$ is also independent of the decay requires the use of very low β thresholds [12]. This is a challenging task in a complex detector such as AIDA. The effect was verified by comparing the P_{1n} values obtained for different ways of reconstructing a β event with different nominal thresholds and sorting conditions. Relative variations of up to 7% were observed when the β efficiency increases

from about 25% to about 40%. The preliminary results so far obtained show a good agreement with previous literature values [34] for ^{76}Cu, ^{77}Cu, ^{79}Zn, ^{80}Zn and ^{82}Ga. Significant differences are observed for ^{78}Cu, ^{81}Zn and ^{82}Zn, and more precise values are obtained for ^{79}Cu and ^{83}Ga. We obtain for the first time P_n values for ^{76}Ni, ^{77}Ni, ^{78}Ni, and ^{80}Cu. Altogether, these results demonstrate the excellent performance of the setup.

In May 2017, the first BRIKEN experiment took place. The measurements in the region around ^{78}Ni and for the formation of the 2$^{\text{nd}}$ r process peak at $A = 130$–140 were completed. A partial measurement for the heaviest elements relevant to the formation of the rare-earth peak was also performed. All three experiments used a ^{238}U beam at 345 MeV/u on a Be target, and the primary beam intensity reached 50 pnA.

As an example of the success of the experiment, we highlight some results from the ^{78}Ni region measurement. Figure 4 displays the combined identification plot of implanted ions for the two BigRIPS settings used. The figure indicates the current limits of measured $T_{1/2}$ and P_n values. In about 95 hours of measurement 6.5 million ions of ^{86}Ge were implanted, a total of 7500 implants were identified as ^{78}Ni ions, and more than 800 ions were collected for the very exotic ^{92}As.

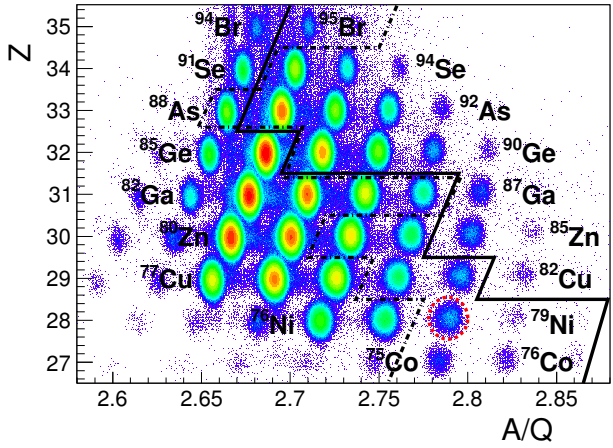

Fig. 4. (Color online) Preliminary particle identification plot (atomic number *versus* mass-over-charge ratio) for the ^{78}Ni region run. The doubly-magic ^{78}Ni is encircled in dotted black/red. The continuum line represents the limit of measured $T_{1/2}$. The dot-dashed line is the limit of measured P_n.

A number of potential $\beta 2n$ emitters were measured for the first time. In order to obtain the P_{2n} value, another spectrum is added to the simultaneous fit. This histogram stores β-implant time differences when two, and only two, neutrons come within Δt_n after the beta. The histogram is corrected for correlated and uncorrelated backgrounds. In addition, the

contribution of two-neutron emission to the one-neutron spectrum, appearing when one of the neutrons escapes detection, is also taken into account. The additional term added to the fit function of Eq. (1) takes the form of $\sum_k \bar{\varepsilon}_\beta^k (\bar{\varepsilon}_n^k)^2 P_{2n}^k \lambda N_k(t)$. As an example, Fig. 5 shows the background corrected spectra of β-implant time differences for one-neutron and two-neutron detection corresponding to the decay of ^{91}As (3.2×10^3 implanted ions) showing the sensitivity of our setup to $\beta 2n$ emission. The analysis of the full set of data is in progress.

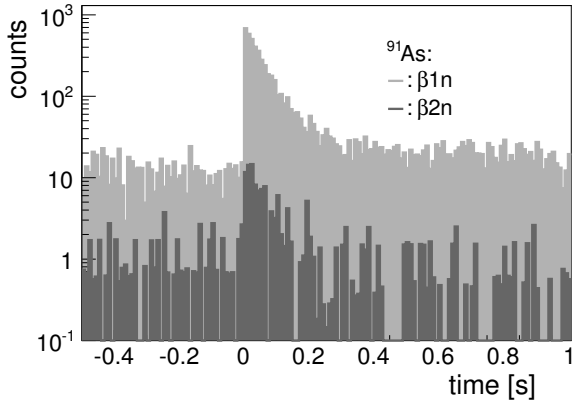

Fig. 5. Time distribution of β signals with respect to implanted ^{91}As ions during the ^{78}Ni region run gated on one-neutron detection (light gray) and two-neutron detection (dark gray).

5. Conclusions and outlook

The BRIKEN setup has been commissioned showing an excellent performance and the first experiments have been performed successfully. The next BRIKEN runs will take place in October–November 2017. During this period, the experiment to study the region of neutron-rich deformed nuclei with $A = 95$–130 will be performed. A second experiment will mainly focus on neutron-gated γ-ray spectroscopy of ^{82}Cu decay to study neutron single-particle levels in the ^{78}Ni region. The measurements to study the formation of the rare-earth peak will be completed in 2018.

Additional experiments are planned in the near future. Three new proposals have been presented. One aims to study the light mass neutron-rich region $Z = 9$–16, $A = 29$–48 that includes a number of potential $\beta 3n$ and $\beta 4n$ emitters. The second one concentrates on the medium-light nuclei $Z = 17$–25, $A = 47$–67 around the shell gaps at $N = 34$ and $N = 40$. The third challenging proposal aims at the heavy region $Z = 72$–83, $A = 190$–224 of importance for the formation of the 3$^{\text{rd}}$ r process peak, whose feasibility at BigRIPS will be investigated.

When completed, this experimental programme will have a major impact on the quantity and quality of decay data for β-delayed neutron emitters, addressing a significant number of key topics in nuclear astrophysics and nuclear structure.

This work has been supported by the Spanish MINECO under grants FPA2011-24553, FPA2011-28770-C03-03, FPA2014-52823-C2-1/2, SEV-2014-0398; by the National Measurement System Programmes Unit of BEIS (UK); by STFC (UK) grant ST/L005743/1; by FP7/EURATOM contract No. 605203; by JSPS KAKENHI grant No. 17H06090; by NSERC grants SAPIN-2014-00028 and RGPAS 462257-2014 at TRIUMF; by the U.S. DOE grant DE-AC05-00OR22725; by the U.S. NSF grant PHY-1714153; by the National Science Centre, Poland (NCN) UMO-2015/18/E/ST2/002. Work partially done within IAEA-CRP for Beta Delayed Neutron Data.

REFERENCES

[1] A. Arcones, G. Martínez-Pinedo, *Phys. Rev. C* **83**, 045809 (2011).

[2] M.R. Mumpower *et al.*, *Prog. Part. Nucl. Phys.* **86**, 86 (2016).

[3] E.M. Burbidge *et al.*, *Rev. Mod. Phys.* **29**, 547 (1957).

[4] D. Kasen *et al.*, *Nature* **551**, 80 (2017).

[5] C. Domingo-Pardo, G. Lorusso, Beta Delayed Neutrons at RIKEN, RIKEN proposal RIBF122, 2013, `https://www.wiki.ed.ac.uk/display/BRIKEN/Home/`

[6] H. Okuno *et al.*, *Prog. Theor. Exp. Phys.* **2012**, 03C002 (2012).

[7] T. Kubo *et al.*, *Prog. Theor. Exp. Phys.* **2012**, 03C003 (2012).

[8] A. Tarifeño-Saldivia *et al.*, *JINST* **12**, 04006 (2017).

[9] R. Grzywacz *et al.*, *Acta Phys. Pol. B* **45**, 217 (2014).

[10] P.L. Reeder *et al.*, *Phys. Rev. C* **15**, 2098 (1977).

[11] M. Bruggeman *et al.*, *Nucl. Instrum. Methods Phys. Res. A* **382**, 511 (1996).

[12] J. Agramunt *et al.*, *Nucl. Instrum. Methods Phys. Res. A* **807**, 69 (2016).

[13] T. Davinson *et al.*, `http://www2.ph.ed.ac.uk/~td/AIDA/`

[14] K.P. Rykaczewski, J.L. Tain, R.K. Grzywacz, I. Dillmann, Measurements of New β-delayed Neutron Emission Properties Around Doubly-magic ^{78}Ni, RIKEN proposal RIBF127, 2015.

[15] S. Nishimura, A. Algora, Decay Properties of r-process Nuclei in Deformed Region Around $A = 100$–125, RIKEN proposal RIBF139, 2015.

[16] A. Estrade, G. Lorusso, F. Montes, Measurement of β-delayed Neutron Emission Probabilities Relevant to the $A = 130$ r-process Abundance Peak, RIKEN proposal RIBF128, 2014.

[17] G.G. Kiss, A.I. Morales, A. Tarifeño, A. Estrade, Masses, Half-lives and β-delayed Neutron Emission Probabilities Relevant to Understand the Formation of the Rare Earth r-process Peak, RIKEN proposal RIBF148, 2016.
[18] P. Möller *et al.*, *Phys. Rev. C* **67**, 055802 (2003).
[19] M. Madurga *et al.*, *Phys. Rev. Lett.* **117**, 092502 (2016).
[20] P. Sarriguren *et al.*, *Phys. Rev. C* **89**, 034311 (2014).
[21] P. Sarriguren, *Phys. Rev. C* **95**, 014304 (2017).
[22] K. Miernik *et al.*, *Phys. Rev. Lett.* **111**, 132502 (2013).
[23] D. Verney *et al.*, *Phys. Rev. C* **95**, 054320 (2017).
[24] J.L. Tain *et al.*, *Phys. Rev. Lett.* **115**, 062502 (2015).
[25] J.L. Tain *et al.*, ND2016, *EPJ Web Conf.* **146**, 01002 (2017).
[26] A. Spyrou *et al.*, *Phys. Rev. Lett.* **117**, 142701 (2016).
[27] B.C. Rasco *et al.*, *Phys. Rev. C* **95**, 054328 (2017).
[28] A. Gottardo *et al.*, *Phys. Lett. B* **772**, 359 (2017).
[29] M.R. Mumpower *et al.*, *Phys. Rev. C* **94**, 064317 (2016).
[30] M. Pfützner *et al.*, *Rev. Mod. Phys.* **84**, 567 (2012).
[31] B. Blank, M.J.G. Borge, *Prog. Part. Nucl. Phys.* **60**, 403 (2008).
[32] R. Caballero-Folch *et al.*, *Phys. Rev. C* **95**, 064322 (2017).
[33] K. Skrable *et al.*, *Health Phys.* **27**, 155 (1974).
[34] `https://www.nndc.bnl.gov/ensdf/`